



Technoeconomic Assessment of Methanol Production Plant Integrated with Solar and Wind Energy Resources in Iraq

Farah A. A. Alkhalidi¹, Yasamin H. Abed², Sahira H. Ibrahim², Erhan Kayabasi^{1,3}, Hasanain A. Abdul Wahhab^{4*}

¹ Mechanical Engineering Department, Karabuk University, 78050 Karabuk, Turkey

² Mechanical Engineering Department, University of Technology, 10066 Baghdad, Iraq

³ Iron and Steel Institute, Karabuk University, 78050 Karabuk, Turkey

⁴ Training and Workshop Center, University of Technology, 35050 Baghdad, Iraq

* Correspondence: Hasanain A. Abdul Wahhab (20085@uotechnology.edu.iq)

Received: 10-19-2025

Revised: 12-25-2025

Accepted: 01-15-2026

Citation: F. A. A. Alkhalidi, Y. H. Abed, S. H. Ibrahim, E. Kayabasi, and H. A. Abdul Wahhab, "Technoeconomic assessment of methanol production plant integrated with solar and wind energy resources in Iraq," *Int. J. Energy Prod. Manag.*, vol. 11, no. 1, pp. 1–16, 2026. <https://doi.org/10.56578/ijepm110101>.



© 2026 by the author(s). Licensee Acadlore Publishing Services Limited, Hong Kong. This article can be downloaded for free, and reused and quoted with a citation of the original published version, under the CC BY 4.0 license.

Abstract: Integration of renewable energy and waste heat resources could effectively reduce emissions and the production cost in methane production power plants. The objective of this study is to conduct a technoeconomic analysis of an Iraqi methanol production facility using a combination of energy resources of waste gas from Al-Fallujah white cement factory, solar and wind energy. It is hypothesized that the carbon dioxide present in the flue gas could be extracted using solar and wind turbine energy in a carbon capture unit in the hydrogen plant. Methanol fuel is then produced in the methanol plant from the combined sources. The amount of energy and the number of solar panels or wind turbines (WT) needed to supply this energy requirement were estimated using the Engineering Equation Solver (EES), and then the environmental impact of the methanol plant was assessed. The efficiencies of renewable energy PV, WT, methanol plants, and methanol fuel were predicted as 21%, 35%, 16.26%, and 58.72%, respectively. The electrolyzers' efficiency was 78.2% at their ideal density of 2.2 kA/m². With a production capacity of 34,530 million tons of methanol, the total cost to operate the plant for 30 years for each of the PV plants and WT was found to be \$9.46 billion and \$5.291 billion, respectively. This translates to 0.4131 \$/kg methane for the PV plant and 0.2413 \$/kg methane for the wind power plant. In terms of the environment, there is a daily 3,894 tons of collected CO₂ emissions and 3,306 tons of mitigation. The results show that the current facility can compete with facilities that produce clean synthetic fuel.

Keywords: Carbon capture; Hybrid energy systems; Hydrogen electrolysis; Methanol production; Solar energy; Wind energy

1 Introduction

Over the past few years, a global emphasis has been on sustainable and eco-friendly energy solutions. This shift is driven by the urgent need to address climate change and transition toward low-carbon economies [1]. As nations worldwide grapple with the profound consequences of conventional fossil fuel usage, the imperative to explore and implement alternative energy sources has gained unprecedented momentum [2]. Within this context, Iraq, endowed with an abundance of solar and wind resources, stands at a pivotal juncture in its quest for sustainable development and energy independence. The country, having historically relied heavily on conventional oil and gas, now faces a unique opportunity to capitalize on its natural resources and diversify its energy portfolio. The endeavor not only aligns with global efforts to transition towards cleaner energy but also positions Iraq as a proactive player in the broader discourse of sustainable development, offering a promising avenue for economic growth while mitigating the environmental impact of traditional energy sources [3]. Al-Kayiem and Mohammed [4] presented an outlook on the utilization of renewable energies in Iraq. One of the proposed ideas is the utilization of solar energy by integration with the existing thermal power plants to reduce the dependence on fossil fuels.

Methanol, a remarkably versatile and pivotal chemical compound, takes center stage in this study due to its multifaceted applications spanning a wide array of industries. With an extensive range of applications, including

being a crucial component in the production of fuels, plastics, and chemicals, methanol stands out for its ability to drive transformative changes in Iraq's industrial landscape. The sheer versatility of methanol is underscored by its role as an essential raw material, contributing significantly to the production of a diverse range of products vital to various sectors [5]. To put its significance into perspective, methanol is utilized in the synthesis of over 50 million metric tons of chemicals annually worldwide. Additionally, it is crucial in producing around 90 million metric tons of formaldehyde, a key ingredient in the manufacturing of resins, plastics, and textiles. Furthermore, methanol is a critical component in the production of adhesives, paints, and pharmaceuticals, further emphasizing its pervasive role in modern industrial processes [6].

As the global community grapples with the imperative to balance economic development with environmental responsibility, methanol emerges as a numerically in the quest for more environmentally friendly and enduring energy solutions. Its production could greatly help in decreasing greenhouse gas emissions, with estimates suggesting that substituting conventional hydrocarbons with methanol can lead to a notable decrease in carbon dioxide emissions by up to 15%. In the context of Iraq's industrial revolution, the strategic decision to harness solar and wind energy for methanol production reflects not only a commitment to meeting the nation's surging energy demands but also a numerical commitment to minimizing its carbon footprint [6].

The integration of solar and wind energy into methanol production serves as a quantifiable step towards achieving sustainable industrial practices, aligning numerical goals with the broader aspirations of environmental conservation and responsible economic growth. By channeling these energies into the intricate processes of methanol production, Iraq has the potential to significantly reduce its carbon footprint, contributing to the global effort to combat climate change [3]. Furthermore, the utilization of indigenous solar and wind resources positions Iraq at the forefront of sustainable energy practices, fostering energy security and resilience against the volatility of fossil fuel markets [7].

Against the backdrop of Iraq's unique energy landscape and its historical reliance on conventional hydrocarbons, this study seeks to unravel the intricate facets of integrating solar and wind energy into the methanol production process. The potential economic ramifications of such a paradigm shift extend beyond the immediate considerations of initial investment and operational efficiency. A thorough investigation is required to assess the long-term economic sustainability, job creation potential, and overall socio-economic impact on the communities surrounding the proposed methanol production plant (MPP). The diversification of Iraq's energy portfolio to include renewable sources not only aligns with the global trajectory toward sustainability but also presents an opportunity for the nation to cultivate a resilient and dynamic energy sector that can withstand the volatility inherent in fossil fuel markets. Additionally, considerations such as maintenance costs, technological advancements, and potential government incentives or subsidies must be factored into the economic feasibility analysis. A comprehensive understanding of these financial intricacies will not only inform the decision-making process for investors and policymakers but also shed light on the potential for cost competitiveness for traditional methanol production methods.

The European Union has recently prioritized the development of new fuels for 2020 to help reduce the pollution from traditional fossil fuels [8]. Despite methanol having nearly half the energy density of gasoline, about 20.1 MJ/kg compared to gasoline's 44.3 MJ/kg, it boasts excellent combustion properties [9]. Using a high compression ratio and adding hydrogen to a lean burn engine fueled by an ethanol-gasoline mix significantly impacts performance and emissions [10]. Methanol has a higher octane rating (108) than gasoline (95), which permits a higher compression ratio, leading to better combustion efficiency and reduced CO and CO₂ emissions compared to conventional gasoline and diesel [9, 11]. Additionally, methanol is crucial for producing various chemicals, including formaldehyde, MTBE, and acetic acid. For these reasons above, methanol production has been subjected to much research in recent years intensively.

For instance, Samimi et al. [12] examined two methods for producing methanol via the reverse water gas shift (RWGS) reaction, focusing on CO₂ conversion. Their findings showed that a membrane reactor using RWGS achieved a higher CO₂ conversion rate and CO yield, along with a more favorable synthesis gas composition due to water removal. Methanol production increased by 50.23% (109 tons/day) compared to the initial scenario and by 4.15% (13 tons/day) compared to a conventional reactor. In a second experiment, methanol synthesis in a reactor resulted in 17% less water production than in the first scenario. Monnerie et al. [13] conducted a techno-economic analysis of a solar thermochemical cycle using cerium oxide to produce H₂ and CO₂. They modeled the process at the system level, utilizing large-scale solar heat to generate synthesis gas (hydrogen and carbon monoxide). Methanol was then produced from this gas in plug-flow reactors without emitting CO₂. The process was simulated in a MW-scale methanol manufacturing facility in Spain, optimized for reactor settings. A cost assessment revealed that a 350 MWh solar plant could produce 27.81 million liters of methanol, requiring 880,685 m² of mirrors and a 220 m solar tower, with an estimated production cost of 1.14 Euros per liter of methanol.

Nizami et al. [14] evaluated two scenarios for methanol production using grid-powered PV electrolysis with and without a battery, focusing on CO₂ hydrogenation. An economic analysis and CO₂ equivalent emissions study assessed environmental impact and economic viability, with levelized costs determined. The overall energy efficiencies were 48.39% for hydrogen generation and 55.16% for methanol synthesis. The cost of methanol

production was found to be \$1,040.17 per ton for the PV-grid scenario and \$1,669.6 per ton for the PV-battery scenario. The PV-grid scenario produced 0.244 kg CO₂-eq/MJ MeOH, while the PV-battery scenario resulted in -0.016 kg CO₂-eq/MJ MeOH. Schorn et al. [15] explored using an energy storage system combining a battery and a power-to-methanol unit for renewable energy storage. They used a nonlinear programming model to determine the minimum-cost capacities for the battery and power-to-methanol units, evaluating four configurations of the renewable energy system. They found that renewable methanol can be cost-competitive with the current fossil market price of 400 €/t under certain conditions. Hydrogen and methanol have comparable energy-specific import costs of 18–30 €/GJ, depending on carbon dioxide prices. The decision to produce methanol at the origin or destination depends on the relative costs of CO₂. If the host country's CO₂ price is 181–228 €/t lower than the origin countries', higher hydrogen shipping expenses can be mitigated.

Sharma et al. [16] proposed using wind energy to electrolyze water, producing hydrogen, and utilizing CO₂ from industrial processes and atmospheric ozone. The process involves combining CO₂ and hydrogen in a reactor to produce methanol and water, with byproducts separated via distillation. Although this method has potential, it faces challenges due to inefficient electrochemical cells and high production costs. The researchers also proposed various wind energy simulations for methanol production, evaluating their feasibility and future potential.

Matzen et al. [17] conducted a techno-economic analysis on a facility that integrates methanol synthesis, CO₂ capture induced by bioethanol, and hydrogen production from wind energy. Using ASPEN Plus software for simulation, the study revealed that the facility produced 97.01 metric tons of methanol daily while consuming 138.37 metric tons of CO₂ and 18.56 metric tons of H₂. The renewable methanol achieved an energy efficiency of approximately 58% and could reduce CO₂ equivalent emissions by -1.05 CO₂ per kilogram of methanol. Bos et al. [18] evaluated the efficiency and capital costs of converting 100 MW of wind power into methanol. The process achieved a power-to-methanol conversion efficiency of 50%. The cost of methanol production was nearly 300 euros per ton without accounting for wind turbine (WT) costs and about 800 euros per ton when including wind turbine costs. The overall facility cost, excluding the wind turbines, was estimated at 200 million euros, with operating costs for electrolyzers, CO₂ capture equipment, and methanol synthesis system at 45%, 50%, and 5%, respectively. The study suggested that producing renewable methanol using CO₂ from the air, water, and renewable electricity is feasible at a cost of 750 to 800 Euros per ton.

Decker et al. [19] explored the short-term integration of systems for electro-fuel production. They listed components for a power-to-fuel system in Germany, including an electrolyzer, hydrogen storage, CO₂ source, wind farm, and synthesis facility, to optimize design parameters and simulate yearly operations. Their model assessed production costs for different scenarios and locations, suggesting that off-grid systems could be viable for short-term implementation. The study indicated that net production costs of methanol could be 1.73 €/IGE, with optimal wind farm sites potentially reducing costs to 1.32 €/IGE. Their methodology and results are also applicable to other regions.

This study embarks on a comprehensive exploration of the techno-economic feasibility of establishing a MPP in Iraq, leveraging the immense potential of solar and wind energy to power the intricacies of the manufacturing processes. In examining the techno-economic aspects of this pioneering approach, key considerations include evaluating the initial investment requirements, operational efficiency, and overall economic viability of a solar and wind-powered MPP in Iraq. This investigation aims to quantify the potential cost savings, resource efficiency gains, and long-term sustainability benefits associated with adopting renewable energy sources for methanol synthesis. Moreover, by scrutinizing the environmental impact, this research seeks to underscore the positive contribution such an initiative can make towards Iraq's commitment to international climate goals and the broader vision of a greener, more sustainable global energy landscape.

2 Materials and Methods

In this study, several factors need to be identified to meet process requirements. These include the temperature and volumetric flow rate of waste gas, the composition of flue gas, the type of renewable energy nearest to the plant, the selection of a CO₂ capture technique from waste gas, the method of composing H₂ gas with carbon atoms, and the choice of suitable software to solve energy and economic equations.

2.1 Plant Properties

The thermodynamic analysis of the White Cement Plant in Fallujah is based on its data and operational conditions. The flue gas has a temperature of 380 °C, a pressure of 1.2 bars, and a flow rate of 126.56 kg/s. The gas composition includes CO₂ (26.2%), CO (0.6%), N₂ (68.8%), and O₂ (4.4%) [20]. The plant is powered by electricity generated from solar panels and WT connected to all its units. To address CO₂ emissions, a post-combustion capture (PCC) unit is used. The Engineering Equation Solver (EES) program was chosen to solve the energy and economic equations. A newly developed method to convert waste gases into valuable products at the White Cement Factory in Al-Faluga has been introduced, aiming to offer a practical solution for advancing green and low-carbon initiatives within the

initiatives of waste-to-wealth and carbon reduction initiatives. The design of a MPP by previous studies has been adopted [20, 21]. Figure 1 shows that the proposed methanol production facility consists of four primary components.

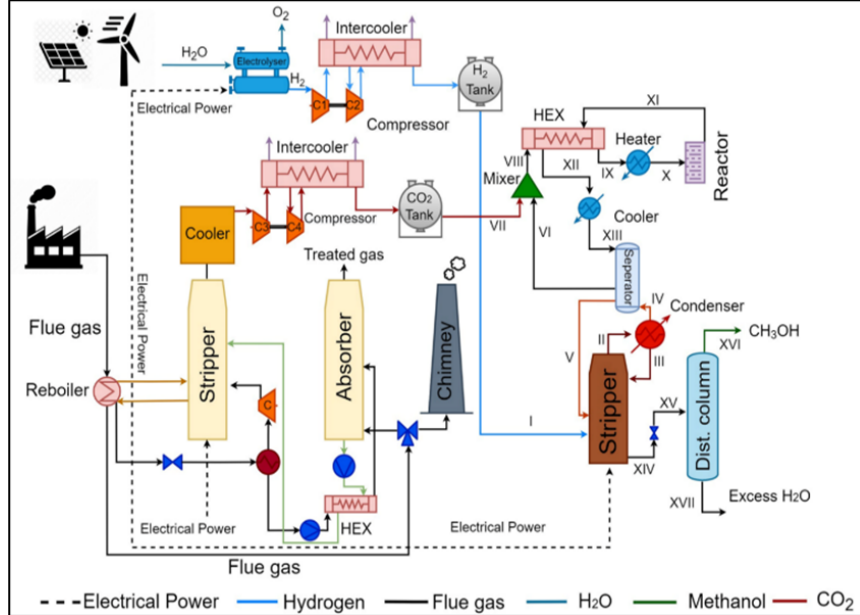


Figure 1. Detailed flow diagram of the methanol production plant

2.2 PV Plant

Table 1. Information regarding the location data [22]

Map Data	Value	Unit
Direct normal irradiation (DNI)	4.905	kWh/m ²
Diffuse horizontal irradiation (DIF)	2.217	kWh/m ²
Global horizontal irradiation (GHI)	5.352	kWh/m ²
Optimal tilt of PV modules (OPTA)	45°	Degree
Global tilted irradiation at optimal angle (GTI OPTA)	6.027	kWh/m ²
Terrain elevation (ELE)	45	m
Air temperature	24.8	°C

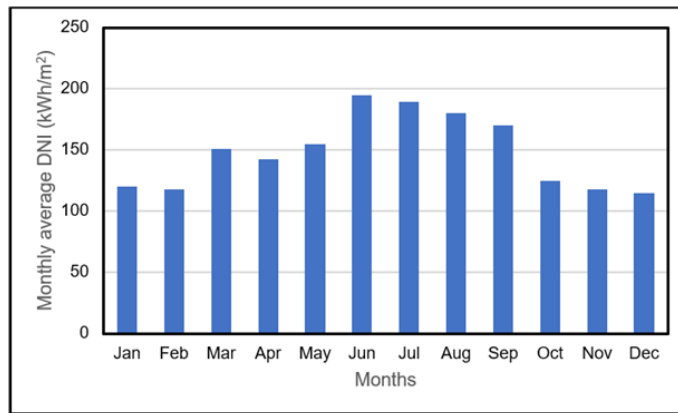


Figure 2. Average monthly levels of direct normal irradiance (DNI) [22]

Solar panels were utilized to produce electricity for the factory. We assumed that large-scale ground-mounted panels would be situated near the factory. These panels cover an area of approximately 1,000 square meters. The

specific location is at coordinates $33^{\circ}22'26.3''$ N, $43^{\circ}50'56.3''$ E, and the data was sourced from the Global Solar Atlas (GSA) as given by the study [22]. Table 1 shows data on the location.

Figure 2 illustrates the monthly mean direct normal irradiance, with peak radiation levels occurring from May through September. Conversely, during the period from October to February, the irradiance rate is lower. Table 2 provides average hourly direct normal irradiance data, including solar radiation rates.

Table 2. Hourly average direct normal irradiation (DNI) in Wh/m^2 [22]

Hours	Jan	Feb	Mar	Apr	May	Jun	Jul	Aug	Sep	Oct	Nov	Dec
5–6	0	0	0	1	24	52	31	2	0	0	0	0
6–7	0	0	22	110	185	281	240	166	102	33	0	0
7–8	53	106	246	275	303	426	387	354	355	245	189	61
8–9	309	316	395	383	414	536	498	471	478	369	392	334
9–10	417	423	497	466	498	616	583	561	571	463	471	431
10–11	490	513	590	533	551	666	633	624	642	540	533	487
11–12	532	559	635	562	575	689	658	650	666	551	552	515
12–13	538	548	617	547	564	687	661	650	655	528	535	511
13–14	507	528	576	505	534	669	645	636	634	490	506	482
14–15	460	473	517	446	476	619	600	587	574	422	446	435
15–16	380	400	438	374	397	540	520	506	480	324	349	339
16–17	111	247	331	281	297	430	410	388	340	117	65	62
17–18	0	11	81	137	179	301	281	208	81	0	0	0
18–19	0	0	0	2	22	59	50	11	0	0	0	0

2.3 Wind Turbine Farm

In the proposed facility, wind energy is harnessed to generate electricity and supply power to the factory. The selected location for the wind turbine farm is Fallujah, Iraq, situated at coordinates $33^{\circ}22'26.3''$ N, $43^{\circ}50'56.3''$ E. Figure 3 illustrates the annual average wind speed [23].

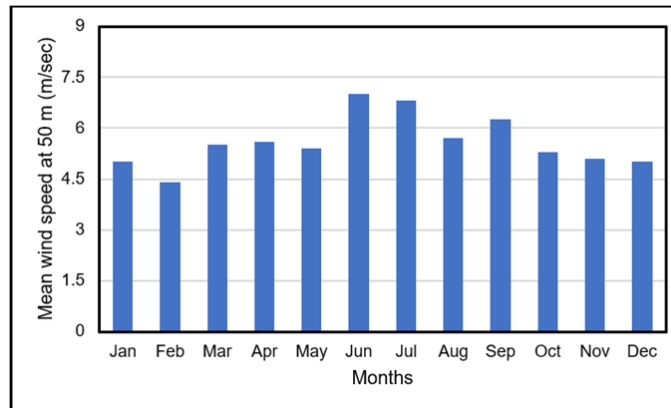


Figure 3. Annual mean wind speed at 50 m height [23]

Table 3. The specifications for the proposed wind turbine

Parameter	Value	Unit	Ref.
Wind speed	3.7	m/s	[4]
Air density	1.25	kg/m ³	[24, 25]
Power Coefficient (C_{P_w})	0.38	–	[24, 25]
Rotor diameter	80	m	[25]
Mechanical efficiency	98	[%]	[24, 25]

The selected WT are 3-blade and the characteristics are shown in Table 3. The selected wind speed represents the site's annual average value.

2.4 Thermodynamic Model

The plant was analyzed using thermodynamic and techno-economic methods. The thermodynamic model was developed and solved using the EES software [20]. The thermophysical properties of the flue gas were obtained from the White Cement Production plant. Energy and mass balances were calculated using Eqs. (1) and (2) [26]:

$$\dot{Q} - \dot{W} = \sum m_{\text{out}} \cdot h_{\text{out}} - \sum m_{\text{in}} \cdot h_{\text{in}} \quad (1)$$

$$\sum \dot{m}_{\text{in}} = \sum \dot{m}_{\text{out}} \quad (2)$$

Heat and work are represented by \dot{Q} and \dot{W} . The thermal efficiency of the plant is determined and calculated by Eq. (3) [27]:

$$\eta = \frac{W_{\text{net}}}{Q_{\text{in}}} \quad (3)$$

Two compressors are used to compress pure CO₂ into the tank. The power for this two-stage process was calculated using the following equations:

$$\dot{W}_{C_3,C_2} = \dot{m}_{CO_2} (h_{2,\text{out}} - h_{1,\text{in}}) \quad (4)$$

$$\dot{W}_{C_4,C_2} = \dot{m}_{CO_2} (h_{4,\text{out}} - h_{3,\text{in}}) \quad (5)$$

The power required by the compressors, denoted as \dot{W} , and the carbon dioxide mass flow rate, represented as \dot{m}_{CO_2} , are essential parameters. A PEM-type electrolyzer operating under conditions of low temperature (400 K) and medium pressure (10000 kPa) has successfully generated hydrogen. By applying Eqs. (6) and (7), one can calculate the power consumption.

$$\dot{W}_{C_1,H_2} = \dot{m}_{H_2} [h_{6,\text{out}} - h_{5,\text{in}}] \quad (6)$$

$$\dot{W}_{C_2,H_2} = \dot{m}_{H_2} [h_{8,\text{out}} - h_{7,\text{in}}] \quad (7)$$

where, \dot{m}_{H_2} represents the hydrogen mass flow rate. The overall cell potential is determined using Eq. (8).

$$E_{\text{tot}} = E_{\text{rev}} + E_{\text{act}} + E_{\text{ohm}} + E_{\text{con}} \quad (8)$$

The terms reversible, activation, ohmic, and concentration are denoted as E_{rev} , E_{act} , E_{ohm} and E_{con} , respectively [28, 29]. Eq. (9) was utilized to calculate the voltage of the cell reversible [30].

$$E_{\text{rev}} = E_o - 85 \times 10^{-4} (T_{\text{cell}} - T_o) + 4.3085 \times (T_{\text{cell}}) \ln \left(\frac{P_{H_2} (P_{O_2})^{0.5}}{P_{H_2O}} \right) \quad (9)$$

$$E_o = -\frac{\Delta G}{zF} \quad (10)$$

In Eq. (10), $-\Delta G$ represents the Gibbs energy associated with the reaction of water splitting, F denotes Faraday's constant, and z signifies the number of electrons transferred. The activation, ohmic, and concentration overpotentials of cell voltage are defined and computed as follows:

$$E_{\text{act}} = \left(\frac{\alpha_a + \alpha_c}{\alpha_a \alpha_c} \right) \frac{RT_{\text{cell}}}{zF} \frac{J}{J_o} \quad (11)$$

R stands for the universal gas constant, T_{cell} indicates the temperature of the cell, α_c and α_a are change coefficients. J_o refers to the exchange current density, defined as follows:

$$J_o = 1.08 \times 10^{-17} \exp(0.086T_{\text{cell}}) \quad (12)$$

The ohmic cell voltage is calculated using Eq. (13).

$$E_{\text{ohm}} = J \frac{t_{\text{mem}}}{\sigma_{\text{mem}}} \quad (13)$$

where, t_{mem} and σ_{mem} represent thickness and membrane conductivity, the cell voltage concentration can be determined by:

$$E_{con} = J \left(\beta \frac{J}{J_c} \right)^\beta \quad (14)$$

where, β denotes a constant related to cell temperature and pressure, while J_c represents the limiting current density [31]. The calculation of the hydrogen rate was performed as follows:

$$\dot{n}_{H_2} = \frac{\dot{W}_{elec}}{E_{tot} \times FZ} \quad (15)$$

To calculate the efficiency of the electrolyzer, we use the following equation:

$$\eta_{elec} = \frac{-DG_t}{E_{tot} \times FZ} \quad (16)$$

The heat load in the components of the methanol plant is determined using the following:

$$\dot{Q}_{heating} = \dot{Q}_{st} + \dot{Q}_{het} + \dot{Q}_{CO2} \quad (17)$$

$$\dot{Q}_{cooling} = \dot{Q}_{dc} + \dot{Q}_{cond} + \dot{Q}_{col} + \dot{Q}_{rea} \quad (18)$$

where, $\dot{Q}_{heating}$ and $\dot{Q}_{cooling}$ represent the utilities for heat and cooling. The terms \dot{Q}_{dc} , \dot{Q}_{st} , \dot{Q}_{cond} , \dot{Q}_{col} , \dot{Q}_{het} and \dot{Q}_{rea} correspond to the heat loads for each component: the distillation column, stripper, condenser, cooler, heater, and reactor, respectively. The fuel efficiency of a MPP can be expressed as follows:

$$\eta_{fuel} = \frac{\frac{m_{45}}{3600} LHV_{met}}{\dot{W}_{Renewable}} \quad (19)$$

The plant efficiency is calculated as follows:

$$\eta_{MP} = \frac{m_{45}h_{45} + m_{46}h_{46}}{(m_{30}h_{30} + m_{36}h_{36} + \dot{W}_{comp,CO2}\dot{W}_{comp,H2}) \times 3600} \quad (20)$$

The factors that determine wind turbine power include [25]:

$$P_{WT} = 0.5 \times C_{p_{w,t}} \times \rho_{air} \times A_{WT} \times U^3 \quad (21)$$

where, ρ_{air} represents air density, while $C_{p_{w,t}}$ denotes the power coefficient of the selected turbine. The latter determines the proportion of wind energy that can be converted into mechanical energy and is capped at a mean value or lower to be on the safe side of 0.38 [25], A corresponds to the rotor area, and U represents wind velocity.

2.5 Technoeconomic Analysis

The initial design of thermal systems needs to consider the investment cost of the system [32]. For this study, a thermodynamic model was developed using EES software. The economic evaluations included not only employment and operational costs but also factors like annual operating time, plant lifespan, interest rates, and maintenance expenses [33].

Each component capital cost rate is referred to as \dot{Z} , and is defined in Eq. (22) [20]:

$$\dot{Z}_{tot,Renewable} = CRF \frac{\phi}{\tau} PEC_{tot,Renewable} \quad (22)$$

In this context, CRF stands for the capital recovery factor, τ denotes the annual operating time, ϕ signifies the maintenance factor, and PEC refers to the equipment purchase cost for each component in the plant. The CRF was determined by Eq. (23):

$$CRF = \frac{i_{eff} (1 + i_{eff})^n}{(1 + i_{eff})^n - 1} \quad (23)$$

An assumed effective interest rate (i_{eff}) of 10% and plant life (n) of 30 years have been considered. The total primary energy consumption $PEC_{\text{tot,Renewable}}$ for both PV plants and WT using Eqs. (24) and (25):

$$PEC_{PV,\text{total}} = PEC_{PV} + PEC_L \quad (24)$$

$$PEC_{WT,\text{total}} = PEC_{WT} \quad (25)$$

where, $PEC_{PV,\text{total}}$, $PEC_{WT,\text{total}}$, PEC_{PV} , PEC_L , PEC_{WT} represent the equipment purchase costs for the PV plant and the WT farm. The cost of the PV plant, PEC_{PV} is calculated based on the rated power P_{PV} , while the cost for the WT, PEC_{WT} is determined by the rated power P_{WT} [34]. The purchase costs for the system components are listed in Table 4.

Table 4. Costs of equipment and components of the proposed system

Components	Cost Correlation	Ref.
PEM electrolyzer	$PEC_{\text{elec}} = 940 \cdot \dot{W}_{\text{electrolyser}}$	[35]
Compressors CO ₂ , H ₂	$PEC_{\text{comp}} = \frac{711 \cdot \dot{m}}{0.9 \cdot \eta_s} \cdot \text{Pr} \cdot \ln(\text{Pr})$	[36]
CCP	$PEC_{\text{ccp}} = \frac{172.95 \cdot \dot{V}_{f,g} \cdot 3600}{10}$	[35]
MPP (Separator and Splitter)	$PEC_{\text{sep}} = \frac{1773 \left(\frac{\text{dailymethanol}}{0.7} \right)}{350}$	[21]
Catalytic Reactor	$PEC_{\text{sep}} = \frac{6582 \left(\frac{\text{dailymethanol}}{0.7} \right)}{350}$	[21]
Distillation Column	$PEC_{\text{sep}} = \frac{4350 \left(\frac{\text{dailymethanol}}{0.7} \right)}{350}$	[21]
PV Panels	$PEC_{PV} = 1500 \times P_{PV}$	[34]
Inverter of PV Panels	$PEC_L = 180 \times P_{PV}$	[34]
Wind Turbine (WT)	$PEC_{WT} = 3500 \times P_{WT}$	[34]

The costs of producing electricity, hydrogen, carbon dioxide, and methanol products are estimated using Eqs. (26)–(29) [20]:

$$\dot{Z}_{\text{elec}} = \frac{\sum \dot{Z}_{\text{tot,Renewable}}}{\dot{W}_{\text{Renewable}}} \quad (26)$$

$$\dot{Z}_{H_2} = \frac{\sum \dot{Z}_{\text{Renewable}} + \sum \dot{Z}_{\text{elec}}}{\dot{m}_{H_2}} \quad (27)$$

$$\dot{z}_{CO_2} = \frac{\sum \dot{z}_{CCP}}{\dot{m}_{CO_2}} \quad (28)$$

$$\dot{z}_{CH_3OH} = \frac{\sum \dot{z}_{\text{Total}}}{\dot{m}_{CH_3OH}} \quad (29)$$

where, $\dot{Z}_{\text{tot,Renewable}}$, \dot{Z}_{elec} , and \dot{Z}_{CCP} denote the overall cost rates of the PV plant, WT turbines, electrolyzer, and carbon capture plant (CCP) respectively, while \dot{Z}_{Total} refers to the total cost rate of the entire plant. The price of electricity is indicated in \$/kWh, whereas other prices are given in units of \$/kg [37].

2.6 Environmental Analysis

Analyzing environmental impacts is essential for quantifying pollutants released into the air. Additionally, reducing emissions can decrease environmental expenses [38, 39]. Hence, procedures to reduce CO₂ must include calculations of total emissions. The carbon emission factors used can vary widely among different types of fuels and even within each type. Natural gas, primarily methane but also containing small amounts of ethane, butane, propane, and other heavier hydrocarbons, has its carbon emission factor influenced by its composition. When natural gas is flared at the production site, it is considered ‘wet’ due to higher levels of non-methane hydrocarbons, further affecting its emission factor. Comparatively, fuels like gasoline, which are less refined than residual fuel oil, generally have lower carbon content per unit of energy. The carbon content of coal per ton depends significantly on its composition of carbon, sulfur, hydrogen, oxygen, ash, and nitrogen. Emissions from all combustion sources are estimated based

on the quantity of fuel used and the average emission factor. The carbon emission factor for coal was determined using the IPCC Tier 1 method, as shown in Eq. (30) [40]:

$$C_C = 32.15 - (0.234 \times H_V) \quad (30)$$

where, C_C represents the carbon emissions factor in tons of carbon per terajoule (tC/TJ), and H_V denotes the gross calorific value of coal, typically ranging from 31 to 37 TJ per kiloton on a dry mineral matter-free basis. The system effectively reduces greenhouse gas (GHG) emissions due to its substantial carbon dioxide consumption. However, reliance on thermal energy results in significant indirect GHG emissions. Eq. (31) can be used to calculate the system's CO₂ reduction capacity.

$$ER_{\text{net}} = ER_{\text{utilization}} - ER_{\text{generation}} \quad (31)$$

where, ER_{net} represents the total CO₂ emissions, $ER_{\text{utilization}}$ denotes the CO₂ utilized within the system's processes, $ER_{\text{generation}}$ indicates the CO₂ produced by the process.

3 Results and Discussion

The efficiency of a methanol plant, η_{MP} , electrolyzer, η_{elec} , fuel efficiency, η_{fuel} , renewable net power, $\dot{W}_{\text{Renewable}}$, purchased equipment costs, PEC, and renewable generation costs, $\dot{Z}_{\text{tot,Renewable}}$ have been determined. Additionally, we examined the costs associated with the methanol plant, methanol production, daily CO₂ capture, and hydrogen production. The calculations were based on data from flue gas measurements at the Fallujah white cement plant. The results and calculated outcomes are presented in the following sections.

3.1 Thermodynamic Analysis

The thermodynamic analysis is essential to understand how the system will operate under specific pressure, temperature, and mass flow conditions. Evaluating the system's performance based on the principles outlined in the first and second laws of thermodynamics is the most effective method. This approach yields detailed insights into the current state of the system. A thermodynamic analysis based on a range of parameters, including varying mass flow rates (from 7,161,000 to 19,820,000 kg/h), enthalpy values (ranging from 6,053 to 2,684 kJ/kg), pressures (from 45 to 1.1 bars), and temperatures (from 443 K to 377.9 K). Additionally, the energy and material balance of the MPP has been examined and detailed in Table 5. The energy duties of the subsystem are summarized in Table 6.

The mass flow of flue gas has a linear impact on the production of hydrogen, methanol, carbon dioxide capture, and emission reduction, as recorded from the control room of the plant, as shown in Figure 4. By rising flue gas levels, it is shown that methanol production rises at the maximum flue gas levels, reaching a maximum of 6,390 tons per day. Also, hydrogen production increases at the highest flue gas rates to 1,358 tons per day. With flue gas levels rising during the process, the amount of carbon dioxide captured rises as well, peaking at 9,962 tons per day. The daily amount of emission reduction at flue gas levels during the process is 9,194 tons per day.

Figure 5 shows the required heat values, where the energy entering the system is considered positive, and the energy leaving the system is negative. The processes in the condenser, cooler, and reactor are exothermic, while the processes in the stripper and distillation column are endothermic.

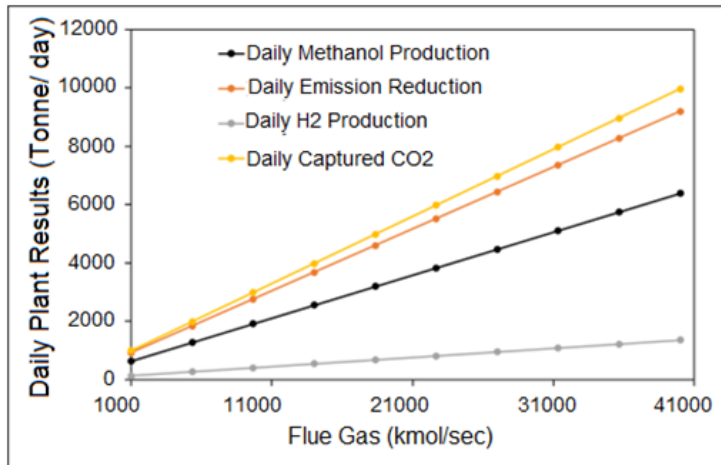


Figure 4. Effects of increasing flue gas on daily operational results

Table 5. Methanol production plant energy and material balance

State	Enthalpy (kJ/kg)	Mass Flow Rate (kg/h)	Pressure (bar)	Temp. (K)
I	6053	22120	45	443
II	2456	33159	45	320
III	-740.6	748.4	45	303
IV	2372	32410	45	303
V	-646.1	175576	45	303
VI	466.4	871803	50	315.1
VII	-264.5	143167	100	293
VIII	381.9	1015000	50	301.2
IX	903.7	1015000	50	498
X	903.7	1015000	50	498
XI	862.4	1015000	50	523
XII	484.6	1015000	50	366.9
XIII	328.1	1015000	50	304
XIV	-465.2	165286	45.2	365.2
XV	-484	165286	5.066	360.6
XVI	-1120	104063	1013	312
XVII	2684	61223	1.1	377.9

Table 6. Energy duties of the plant

Component	Value
Carbon capture plant (CCP)	
CCP heat load	32770 kW
CCP workload	4055 kW
Hydrogen production	
Daily H ₂ production	530874 kg/day
Cell voltage	1.57 V
Methane production plant (MPP)	
CO ₂ compressor power	10561 kW
H ₂ compressor power	444.71 kW
Cooler heat duty	-44111 kW
Reactor heat duty	-11656 kW
Distillation column heat duty	35508 kW
Stripper heat duty	4262 kW
Condenser heat duty	-1423 kW
Daily methanol production	2498 ton/day

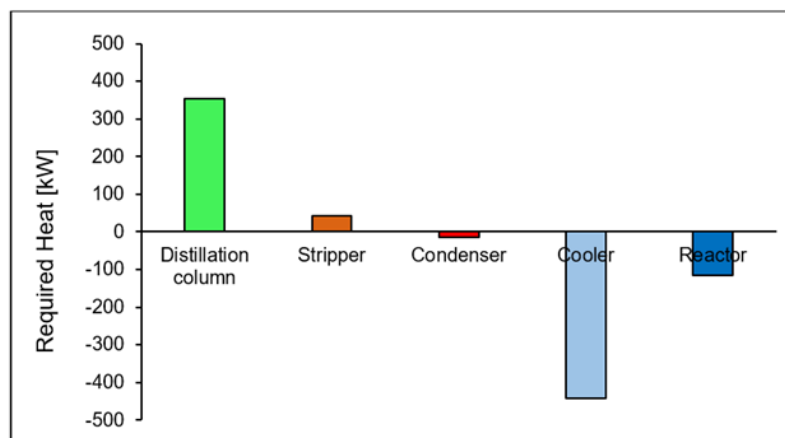


Figure 5. The required heat for each unit in the methane power plant

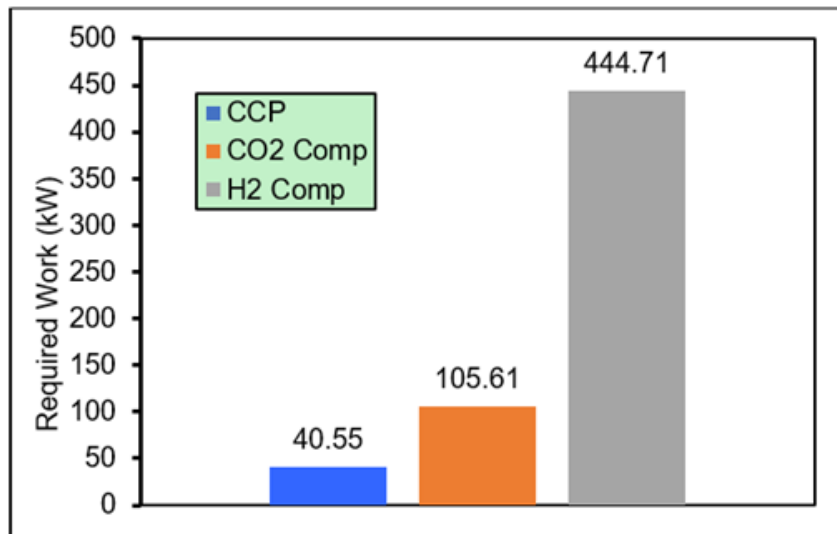


Figure 6. The required work for the unit in the system

Based on the required work prediction, shown in Figure 6, compressors used for hydrogen production are shown to have the greatest work input demand, with a value of 444.71 kW. This amount is more than twice the necessary business input requirements of both the carbon dioxide compressors and the CCP combined.

3.2 Technoeconomic Analysis

The cost analysis for each product and the annual operating expenses of the plant are determined through a component-based approach. Thermodynamic analysis results guide cost calculations, treating power-consuming and energy-producing components as functions of their energy consumption or production.

Additionally, the plant size impacts the costs associated with the CCP and MPP. The key findings of the economic study are summarized in Table 7.

Table 7. Cost prediction of each component or production method based on the developed economic analysis model

Parameter	Value	Unit
Renewable cost (PV)	1.955	M \$/y
Renewable cost (WT)	70.350	M \$/y
Electricity cost (PV)	0.02851	\$/kWh
Electricity cost (WT)	0.01026	\$/kWh
Carbon capture plant cost (CCP)	1.228	M \$/y
Electrolyser cost	104	M \$/y
CO ₂ production cost	0.0016	\$/kg
Hydrogen production cost (PV)	1.936	\$/kg
Hydrogen production cost (WT)	1.127	\$/kg
Methanol production plant cost (MPP)	790.825	\$/y
Methanol production cost (PV)	0.4131	\$/kg
Methanol production cost (WT)	0.2413	\$/kg

Figure 7 illustrates the declining cost of the plant throughout its lifespan. For instance, at the 30-year mark (the considered lifespan), the PV plant costs \$9.46 billion, and the wind plant costs \$5.291 billion. By the 40-year mark, the PV plant's value is approximately \$8.72 billion, while the wind plant's value is around \$5.1 billion.

Figure 8 shows the area of the PV panels, the wind plant, and the cost of equipment for the PV panels and the wind plant versus levels of flue gas at 40,000 (kmol/s), where the maximum area of the PV panels is 104,500 m², the wind plant is 682,000 m², and the maximum cost is \$4,211 billion and \$1,515 billion, respectively.

Figure 9 shows the total cost of the wind turbine ($\dot{Z}_{tot,WT}$) and the total cost of the PV panels ($\dot{Z}_{tot,PV}$), the total cost of methanol by wind turbine ($\dot{Z}_{Methanol,WT}$) and the total cost of the methanol by PV panels ($\dot{Z}_{Methanol,PV}$) as the plant's life changes, at the 30th point of the plant's life, being \$2.811 per second, \$7.712 per second, \$0.243 per kg, and \$0.4106 per kg, respectively indicating that costs decrease with an increase in the plant's life.

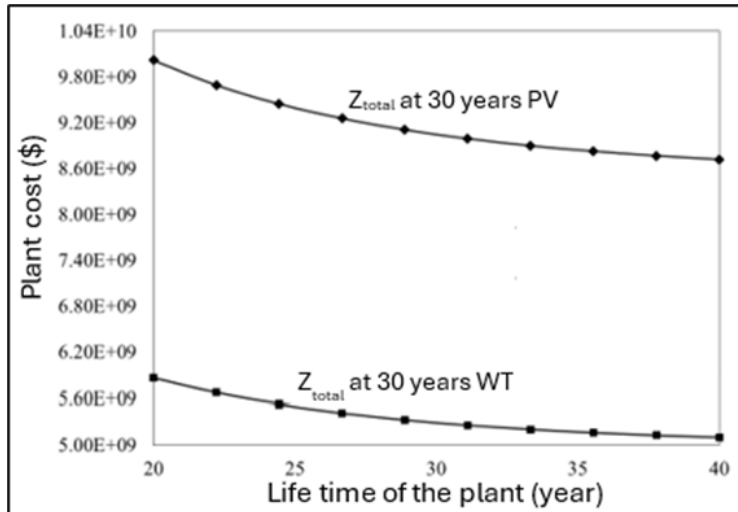


Figure 7. Effects of increasing the life cycle of the plant on production costs

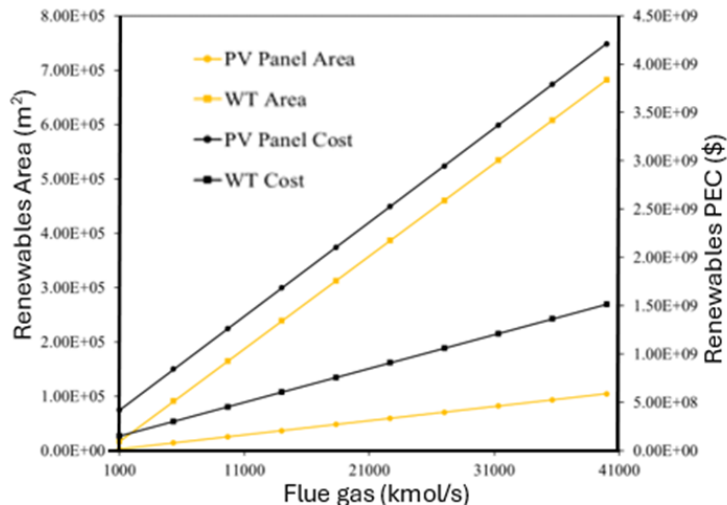


Figure 8. Effects of increased flue gas on renewables area and renewables purchase equipment cost

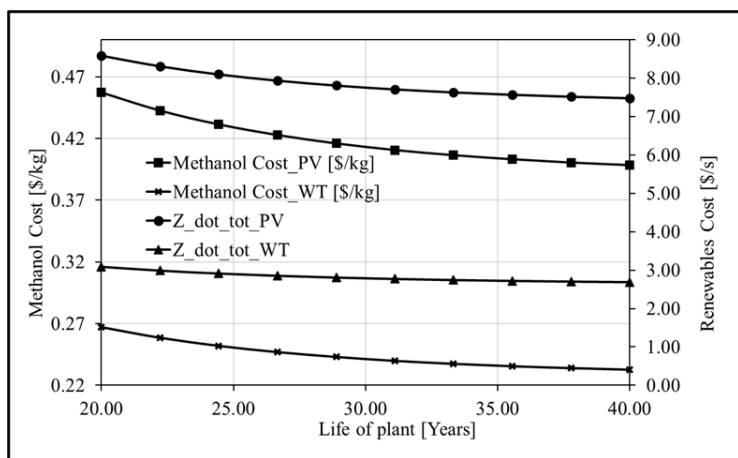


Figure 9. Effects of increased plant life on methanol costs and total wind turbine PV panel costs

When Figure 10 is assessed, it is seen that the highest PEC is the PV plant. This is because the PV panel area required for the electrolysis of hydrogen, which corresponds to the mass flow rate of hydrogen retained carbon dioxide, is very high. This cost may decrease in the near future with advances in technology and the production

of new-generation PV panels that provide higher energy production from less space. Secondly, the highest PEC is observed in the hydrogen plant. This is an expected situation where, as in the PV panel, the energy required for the electrolysis of hydrogen increases linearly with the amount of hydrogen that will react with carbon dioxide. There may be decreases in PEC as alternative methods and new generation technologies for hydrogen production are developed, and their use becomes widespread in the near future. Maintenance and repair costs and initial investment costs in WT are higher than in PV panels. However, in regions where the permissible solar panel area and the amount of radiation are low, WT stand out as a very good alternative. In this study, PV electricity and wind energy were evaluated as alternatives to each other, and it is observed that WT are more advantageous for the selected region.

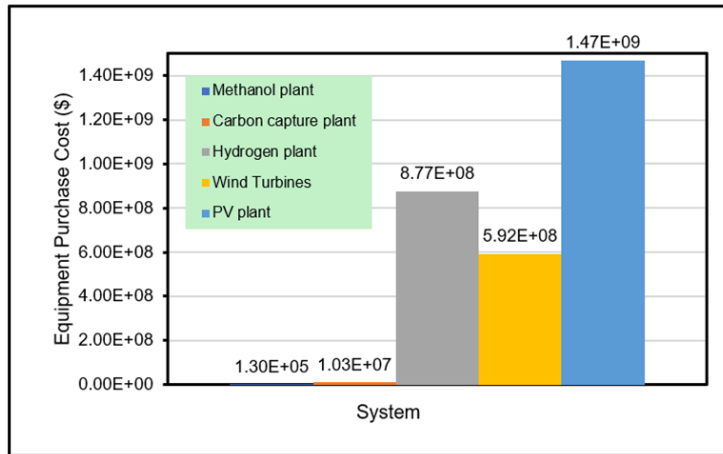


Figure 10. Outlook of the overall system's purchase equipment cost

3.3 Environmental Analysis

In this section, we explore the calculated CO₂ emissions from the production plant and methods for mitigating them. Figure 4 illustrates the correlation between flue gas levels and emission reduction. At the highest flue gas level, the most significant reduction in emissions amounts to 9194 tons per day. The fact that daily emission reduction increases with increasing flue gas suggests that the process includes a technology to capture emissions that is becoming more efficient as the amount of flue gas increases, where the amount of carbon dioxide captured reached 9962 tons per day in this process. Consequently, it is possible to significantly reduce carbon emissions caused by a cement factory's waste flue gas.

4 Conclusion

This research conducts a thorough analysis of the economic and environmental aspects involved in operating a methanol production facility that utilizes solar and wind power alongside waste gases from a white cement plant. Below are the key findings of the study:

1. It estimates that 3,894 tons of CO₂ can be captured daily, with a heating load of 32,770 kW for the carbon capture process in the case where the H/C ratio has been assumed to be stoichiometric.
2. Under ideal reactor conditions, approximately 2,498 tons of methanol can be produced daily.
3. The PEM electrolyzer cell achieves a maximum efficiency of 0.782% at a 400 K cell temperature and 2.2 kA/m² current density, resulting in a daily hydrogen production rate of 530,874 kg.
4. The overall efficiency of the plant is calculated to be 0.163%, while the MPP fuel efficiency is 0.587%.
5. The total 30-year operational costs for PV and wind turbine plants are \$9.46 billion and 5.291 billion, respectively. This investment could yield over 34,530 million tons of methanol, costing approximately 0.4131 kg of methane for the PV plant and 0.2413 \$/kg for the WT plant.
6. The captures amount to approximately 3,894 tons of emissions daily, with a mitigation rate of around 3,306 tons per day.

Data Availability

The data used to support the findings of this study are available from the corresponding author upon request.

Acknowledgment

The authors acknowledge the University of Technology, Baghdad, Iraq, for the technical support to conduct the research by providing all requirements.

Conflicts of Interest

The authors declare that they have no conflicts of interest.

References

- [1] S. Bakhsh, W. Zhang, K. Ali, and M. Anas, “Energy transition and environmental stability prospects for OECD economies: The prominence role of environmental governance, and economic complexity: Does the geopolitical risk matter,” *J. Environ. Manag.*, vol. 354, p. 120358, 2024. <https://doi.org/10.1016/j.jenvman.2024.120358>
- [2] Q. Hassan, P. Viktor, T. J. Al-Musawi, and B. Mahmood Ali, “The renewable energy role in the global energy transformations,” *Renew. Energy Focus*, vol. 48, p. 100545, 2024. <https://doi.org/10.1016/j.ref.2024.100545>
- [3] M. T. Chaichan and H. A. Kazem, *Generating Electricity Using Photovoltaic Solar Plants in Iraq*. Springer, Cham, 2018. <https://doi.org/10.1007/978-3-319-75031-6>
- [4] H. H. Al-Kayiem and S. T. Mohammad, “Potential of renewable energy resources with emphasis on solar power in Iraq: An outlook,” *Resources*, vol. 8, no. 1, p. 42, 2019. <https://doi.org/10.3390/resources8010042>
- [5] S. V. Valentine, “Emerging symbiosis: Renewable energy and energy security,” *Renew. Sustain. Energy Rev.*, vol. 15, no. 9, pp. 4572–4578, 2011. <https://doi.org/10.1016/j.rser.2011.07.095>
- [6] A. F. Kareem, A. Akroot, H. A. Abdul Wahhab, W. Talal, R. M. Ghazal, and A. Alfaris, “Exergo-economic and parametric analysis of waste heat recovery from Taji gas turbines power plant using Rankine cycle and organic Rankine cycle,” *Sustainability*, vol. 15, no. 12, p. 9376, 2023. <https://doi.org/10.3390/su15129376>
- [7] H. A. Abdul Wahhab, S. Aljabair, and S. K. Ayed, “Assessment of wind fin performance run by mixed flows: Experimental and numerical investigation,” *Arab. J. Sci. Eng.*, vol. 46, no. 12, pp. 12 077–12 088, 2021. <https://doi.org/10.1007/s13369-021-05843-w>
- [8] L. A. Al-Azez Mahdi, S. A. Mahmood, M. K. J. Al-naamee, M. A. Fayad, M. T. Chaichan, and H. A. Abdul Wahhab, “Thermal analysis of wire on tube condenser by exergy and penalty factor methods,” in *Advances in Material Science and Engineering: Selected Articles from ICMMPE 2023*, Putrajaya, Malaysia, 2023, pp. 127–141. https://doi.org/10.1007/978-981-97-2015-6_11
- [9] D. Suresh and E. Porpatham, “Influence of high compression ratio on the performance of ethanol-gasoline fuelled lean burn spark ignition engine at part throttle condition,” *Case Stud. Therm. Eng.*, vol. 53, p. 103832, 2024. <https://doi.org/10.1016/j.csite.2023.103832>
- [10] H. Valera and A. K. Agarwal, “Methanol as an alternative fuel for diesel engines,” in *Methanol and the Alternate Fuel Economy*. Springer, Singapore, 2019, pp. 9–33. https://doi.org/10.1007/978-981-13-3287-6_2
- [11] I. Veza, Irianto, A. T. Hoang, and A. A. Yusuf, “Effects of Acetone-Butanol-Ethanol (ABE) addition on HCCI-DI engine performance, combustion and emission,” *Fuel*, vol. 333, no. Part 1, p. 126377, 2023. <https://doi.org/10.1016/j.fuel.2022.126377>
- [12] F. Samimi, N. Hamedi, and M. R. Rahimpour, “Green methanol production process from indirect CO₂ conversion: RWGS reactor versus RWGS membrane reactor,” *J. Environ. Chem. Eng.*, vol. 7, no. 1, p. 102813, 2019. <https://doi.org/10.1016/j.jece.2018.102813>
- [13] N. Monnerie, P. G. Gan, M. Roeb, and C. Sattler, “Methanol production using hydrogen from concentrated solar energy,” *Int. J. Hydrot. Energy*, vol. 45, no. 49, pp. 26 117–26 125, 2020. <https://doi.org/10.1016/j.ijhydene.2019.12.200>
- [14] M. Nizami, Slamet, and W. W. Purwanto, “Solar PV based power-to-methanol via direct CO₂ hydrogenation and H₂O electrolysis: Techno-economic and environmental assessment,” *J. CO₂ Util.*, vol. 65, p. 102253, 2022. <https://doi.org/10.1016/j.jcou.2022.102253>
- [15] F. Schorn, J. L. Breuer, R. C. Samsun, and T. Schnorbus, “Methanol as a renewable energy carrier: An assessment of production and transportation costs for selected global locations,” *Adv. Appl. Energy*, vol. 3, p. 100050, 2021. <https://doi.org/10.1016/j.adopen.2021.100050>
- [16] I. Sharma, V. Shah, and M. Shah, “A comprehensive study on the production of methanol from wind energy,” *Environ. Technol. Innov.*, vol. 28, p. 102589, 2022. <https://doi.org/10.1016/j.eti.2022.102589>
- [17] M. Matzen, M. Alhajji, and Y. Demirel, “Chemical storage of wind energy by renewable methanol production: Feasibility analysis using a multi-criteria decision matrix,” *Energy*, vol. 93, no. Part 1, pp. 343–353, 2015. <https://doi.org/10.1016/j.energy.2015.09.043>
- [18] M. J. Bos, S. R. A. Kersten, and D. W. F. Brilman, “Wind power to methanol: Renewable methanol production using electricity, electrolysis of water, and CO₂ air capture,” *Appl. Energy*, vol. 264, p. 114672, 2020. <https://doi.org/10.1016/j.apenergy.2020.114672>
- [19] M. Decker, F. Schorn, R. C. Samsun, and R. Peters, “Off-grid power-to-fuel systems for a market launch

- scenario – A techno-economic assessment,” *Appl. Energy*, vol. 250, pp. 1099–1109, 2019. <https://doi.org/10.1016/j.apenergy.2019.05.085>
- [20] H. Ozcan and E. Kayabasi, “Thermodynamic and economic analysis of a synthetic fuel production plant via CO₂ hydrogenation using waste heat from an iron-steel facility,” *Energy Convers. Manag.*, vol. 236, p. 114074, 2021. <https://doi.org/10.1016/j.enconman.2021.114074>
- [21] A. A. Kiss, J. J. Pragt, H. J. Vos, and G. Bargeman, “A novel efficient process for methanol synthesis by CO₂ hydrogenation,” *Chem. Eng. J.*, vol. 284, pp. 260–269, 2016. <https://doi.org/10.1016/j.cej.2015.08.101>
- [22] A. C. Brent, J. Hinkley, D. Burmester, and R. Rayudu, “Solar atlas of New Zealand from satellite imagery,” *J. R. Soc. N. Z.*, vol. 50, no. 4, pp. 572–583, 2020. <https://doi.org/10.1080/03036758.2020.1763409>
- [23] NASA Prediction of Worldwide Energy Resources, “NASA POWER — Data Access Viewer,” 2024. <https://power.larc.nasa.gov/data-access-viewer/>
- [24] C. Jung and D. Schindler, “Efficiency and effectiveness of global onshore wind energy utilization,” *Energy Convers. Manag.*, vol. 280, p. 116788, 2023. <https://doi.org/10.1016/j.enconman.2023.116788>
- [25] O. Oner and I. Dincer, “Development and assessment of a hybrid biomass and wind energy-based system for cleaner production of methanol with electricity, heat, and freshwater,” *J. Clean. Prod.*, vol. 367, p. 132967, 2022. <https://doi.org/10.1016/j.jclepro.2022.132967>
- [26] A. Atmaca and R. Yumrutas, “Thermodynamic and exergoeconomic analysis of a cement plant: Part I – Methodology,” *Energy Convers. Manag.*, vol. 79, pp. 790–798, 2014. <https://doi.org/10.1016/j.enconman.2013.11.053>
- [27] A. Mohammadi, M. Ashouri, M. H. Ahmadi, and M. Bidi, “Thermoeconomic analysis and multiobjective optimization of a combined gas turbine, steam, and organic Rankine cycle,” *Energy Sci. Eng.*, vol. 6, no. 5, pp. 506–522, 2018. <https://doi.org/10.1002/ese3.227>
- [28] A. Reinders, P. J. Verlinden, W. Van Sark, and A. Freundlich, *Photovoltaic Solar Energy: From Fundamentals to Applications*. John Wiley & Sons, 2017.
- [29] D. Bessarabov, H. Wang, H. Li, and N. Zhao, *PEM Electrolysis for Hydrogen Production: Principles and Applications*. CRC Press, 2016.
- [30] H. C. Zhang, S. H. Su, G. X. Lin, and J. C. Chen, “Efficiency calculation and configuration design of a PEM electrolyzer system for hydrogen production,” *Int. J. Electrochem. Sci.*, vol. 7, no. 5, pp. 4143–4157, 2012. [https://doi.org/10.1016/S1452-3981\(23\)19527-7](https://doi.org/10.1016/S1452-3981(23)19527-7)
- [31] O. Kumar and S. C. Kaushik, “Energy and exergy analysis and optimization of Kalina cycle coupled with a coal-fired steam power plant,” *Appl. Therm. Eng.*, vol. 51, no. 1-2, pp. 787–800, 2013. <https://doi.org/10.1016/j.applthermaleng.2012.10.006>
- [32] Q. Zhang, Z. W. Luo, Y. J. Zhao, and R. Cao, “Performance assessment and multi-objective optimization of a novel transcritical CO₂ trigeneration system for a low-grade heat resource,” *Energy Convers. Manag.*, vol. 204, p. 112281, 2020. <https://doi.org/10.1016/j.enconman.2019.112281>
- [33] B. Besevli, E. Kayabasi, A. Akroot, and W. Talal, “Technoeconomic analysis of oxygen-supported combined systems for recovering waste heat in an iron-steel facility,” *Appl. Sci.*, vol. 14, no. 6, p. 2563, 2024. <https://doi.org/10.3390/app14062563>
- [34] A. Buonomano, F. Calise, M. D. d’Accadia, and M. Vicidomini, “A hybrid renewable system based on wind and solar energy coupled with electrical storage: Dynamic simulation and economic assessment,” *Energy*, vol. 155, pp. 174–189, 2018. <https://doi.org/10.1016/j.energy.2018.05.006>
- [35] A. Tozlu, “Techno-economic assessment of a synthetic fuel production facility by hydrogenation of CO₂ captured from biogas,” *Int. J. Hydrot. Energy*, vol. 47, no. 5, pp. 3306–3315, 2022. <https://doi.org/10.1016/j.ijhydene.2020.12.066>
- [36] A. Tozlu, A. Abuoğlu, and E. Özahi, “Thermoeconomic analysis and optimization of a re-compression supercritical CO₂ cycle using waste heat of gaziantep municipal solid waste power plant,” *Energy*, vol. 143, pp. 168–180, 2018. <https://doi.org/10.1016/j.energy.2017.10.120>
- [37] A. Akroot, M. Almaktar, and F. Alasali, “The integration of renewable energy into a fossil fuel power generation system in oil-producing countries: A case study of an integrated solar combined cycle at the Sarir power plant,” *Sustainability*, vol. 16, no. 11, p. 4820, 2024. <https://doi.org/10.3390/su16114820>
- [38] F. L. Lu, Y. Zhu, M. Z. Pan, and C. Li, “Thermodynamic, economic, and environmental analysis of new combined power and space cooling system for waste heat recovery in waste-to-energy plant,” *Energy Convers. Manag.*, vol. 226, p. 113511, 2020. <https://doi.org/10.1016/j.enconman.2020.113511>
- [39] B. Saadatfar, R. Fakhrai, and T. Fransson, “Exergo-environmental analysis of nanofluid ORC low-grade waste heat recovery for hybrid trigeneration system,” *Energy Procedia*, vol. 61, pp. 1879–1882, 2014. <https://doi.org/10.1016/j.egypro.2014.12.233>

- [40] IPCC, “Energy,” in *Revised 1996 IPCC Guidelines for National Greenhouse Gas Inventories: Reference Manual (Volume 3)*, 1996, pp. 1–40. <https://www.ipcc-nggip.iges.or.jp/public/gl/lnvs6a.html>